

Supplementary Information

Insight into Lithium-metal Anode in Lithium-Sulfur Batteries with a Fluorinated Ether Electrolyte

Chenxi Zu,^[a] Nasim Azimi,^{[b][c]} Zhengcheng Zhang,^[b] and Arumugam Manthiram*^[a]

[a] Materials Science and Engineering, Texas Materials Institute, The University of Texas at Austin, Austin, Texas 78712, United States

[b] Chemical Sciences and Engineering Division, Argonne National Laboratory, 9700 S. Cass Avenue, Lemont, IL 60439, United States

[c] Departments of Chemical Engineering and Bioengineering, University of Illinois at Chicago, Chicago, IL 60607, United States

Corresponding Author

E-mail: manth@austin.utexas.edu

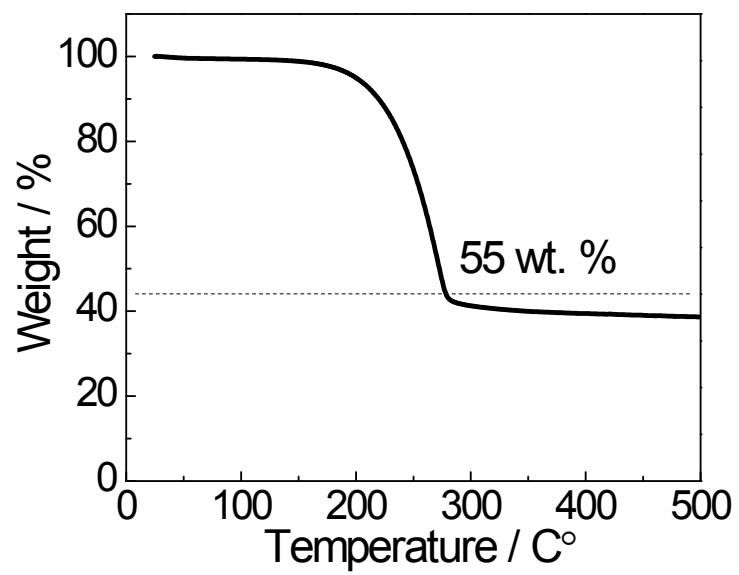


Figure S1. TGA plot of the GS composite.

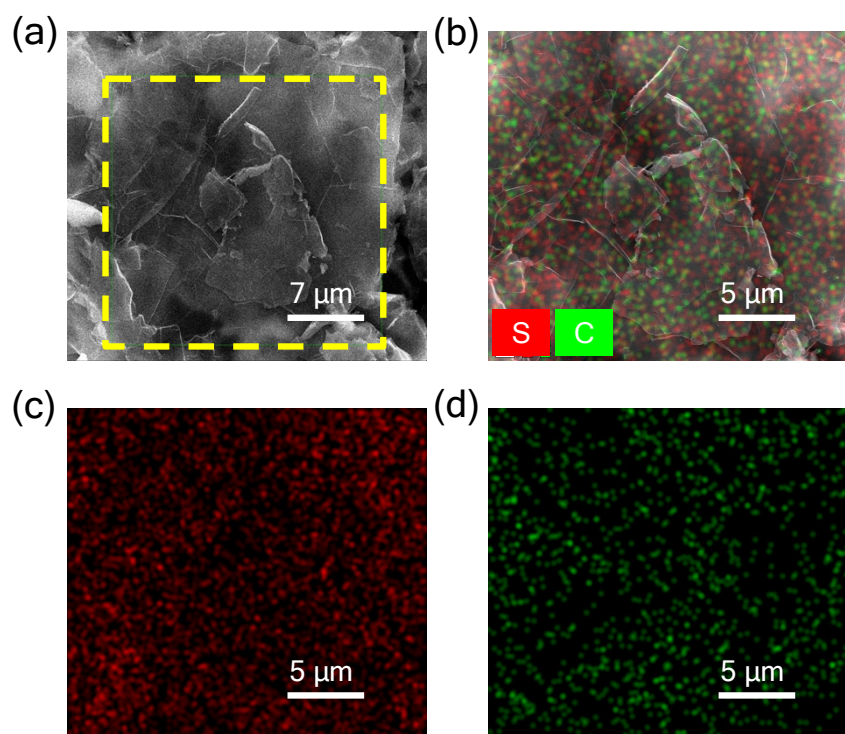


Figure S2. SEM image (a) and EDS elemental mappings (b; c; d) of the GS composite. Sulfur and carbon signals are indicated, respectively, in red and green.

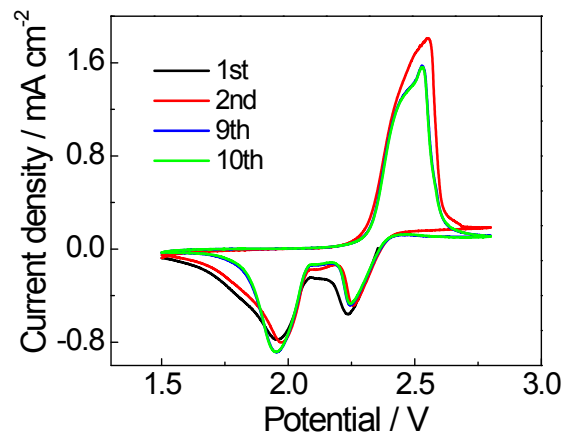


Figure S3. CV profile of the GS-DOL/DME-Li cell.

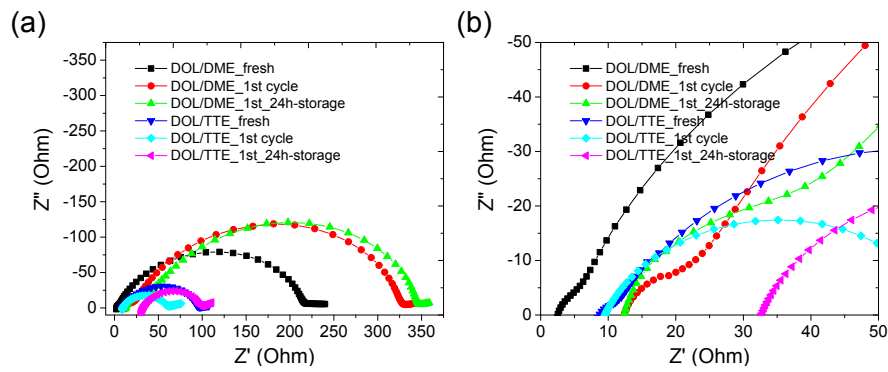


Figure S4. (a) EIS data of the Li-DOL/DME-Li symmetric cell and Li-DOL/TTE-Li symmetric cell after the fresh assembly, after the first cycle, and after the first cycle and the following 24h-storage. The major semicircle shown in (a) represents the charge-transfer resistance. (b) Magnified EIS plot of (a), showing the intersection between the initial part of the high frequency semicircle and the real axis. The intersection represents the electrolyte resistance. It can be seen that DOL/TTE electrolyte has higher resistance than DOL/DME electrolyte after the fresh assembly.

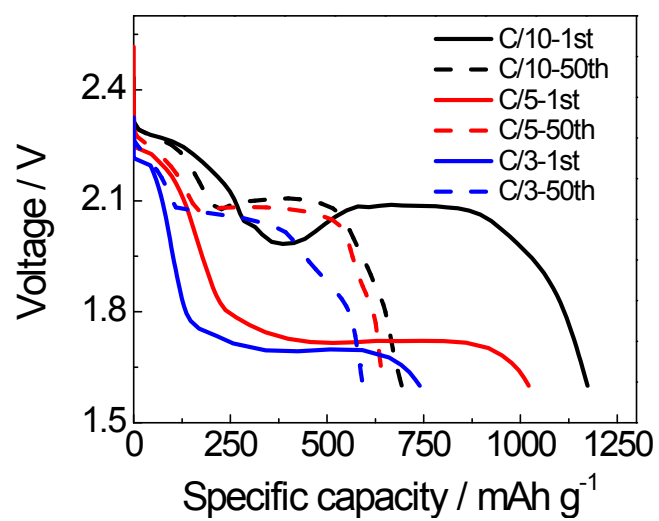


Figure S5. Discharge voltage profiles of the GS-DOL/TTE-Li cell at C/10, C/5, and C/3 rates.

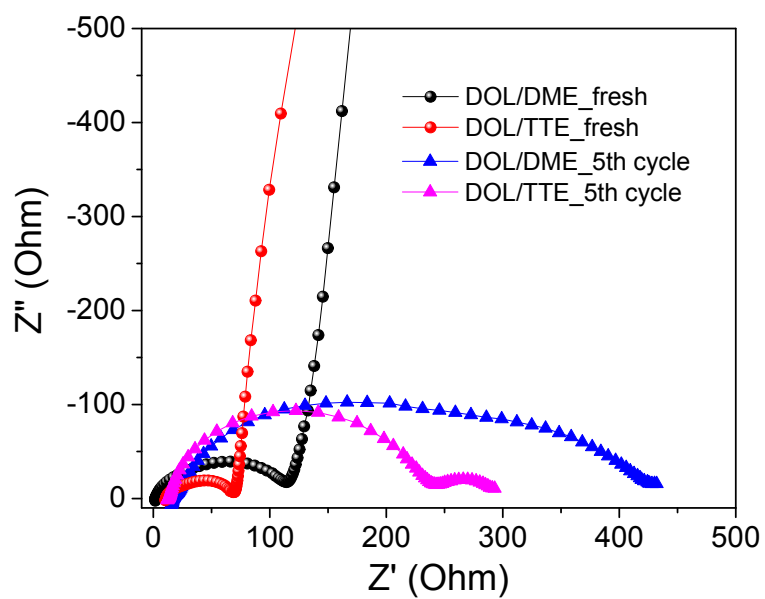


Figure S6. EIS data of the pure sulfur cathode-DOL/DME-Li cell and pure sulfur cathode-DOL/TTE-Li cell after the fresh assembly and after the 5th cycle. Conventional sulfur cathodes with 70 wt. % sulfur, 20 wt. % super P conductive carbon, and 10 wt. % polyvinylidene fluoride (PVDF) binder are used.

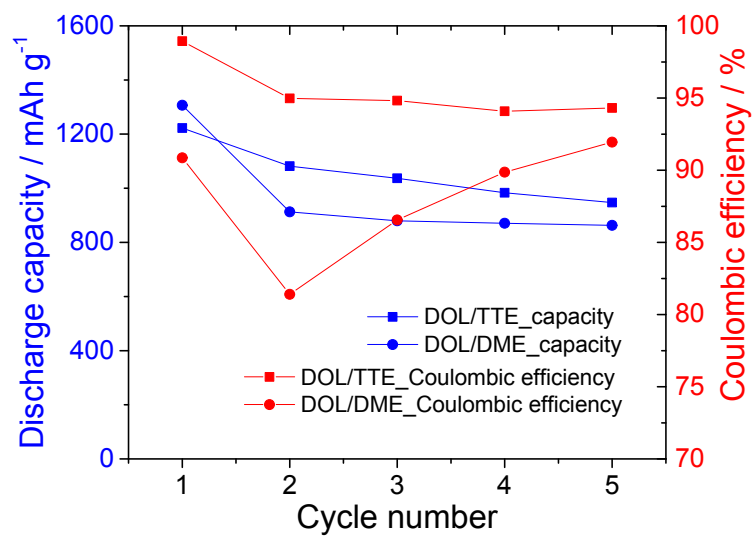


Figure S7. Discharge capacity and Coulombic efficiencies of the pure sulfur cathode-DOL/DME-Li cell and pure sulfur cathode-DOL/TTE-Li cell. Conventional sulfur cathodes with 70 wt. % sulfur, 20 wt. % Super P conductive carbon, and 10 wt. % polyvinylidene fluoride (PVDF) binder are used. The cells were cycled at C/5.

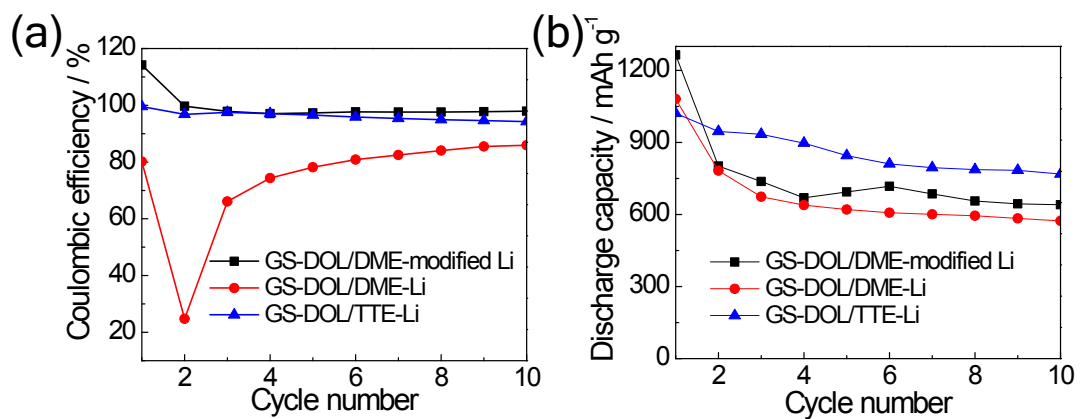


Figure S8. (a) Coulombic efficiencies and (b) cycling performances of the GS-DOL/DME-modified Li, GS-DOL/DME-Li, and GS-DOL/TTE-Li cells.

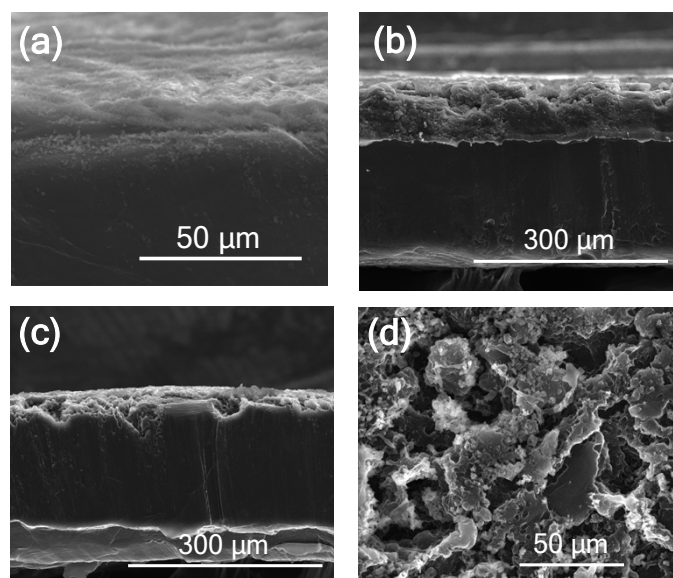


Figure S9. Cross-sectional SEM images showing the lithium-metal anode cycled in (a) DOL/TTE electrolyte after the first charge, (b) DOL/TTE electrolyte after the 50th charge, and (c) DOL/DME electrolyte after the 50th charge at C/5. (d) Front-view SEM image of the lithium-metal anode cycled in DOL/DME electrolyte **after 50 cycles**.

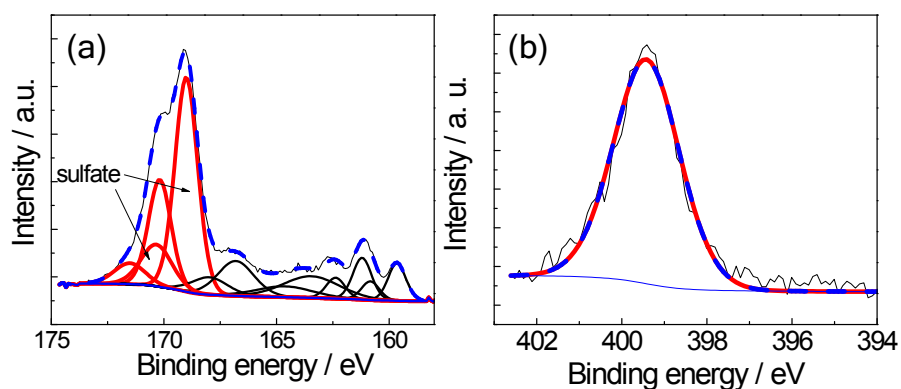


Figure S10. (a) XPS S 2p region of the lithium-metal anode cycled in DOL/TTE electrolyte before sputtering. (b) XPS N 1s region of the lithium-metal anode cycled in DOL/TTE electrolyte before sputtering. XPS peak area fitting using the CasaXPS software indicates the molar ratio between S from sulfate and N is 43/29 instead of 2:1 as in LiTFSI.

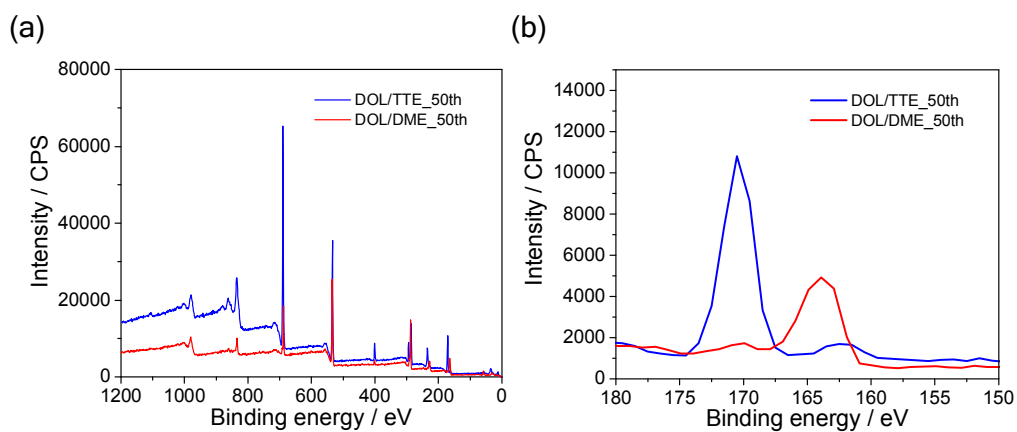


Figure S11. (a) XPS survey of the lithium-metal anode cycled in DOL/TTE electrolyte and DOL/DME electrolyte for 50 cycles; (b) magnified image showing the sulfur region in (a).

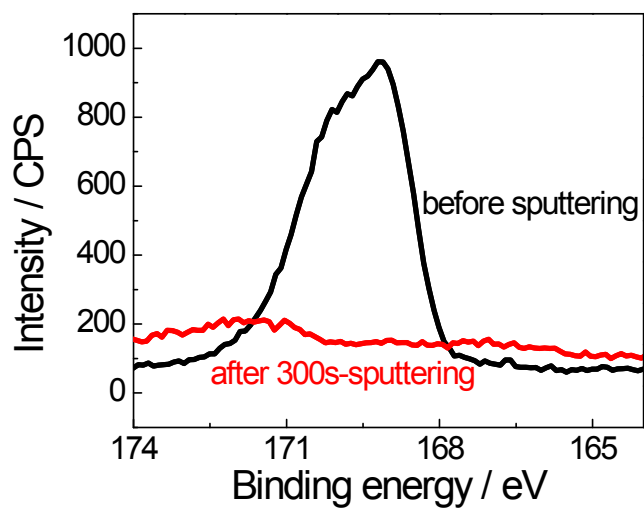


Figure S12. XPS S 2p region spectra of the lithium-metal anode rinsed with DOL/TTE electrolyte with 1 M LiTFSI.

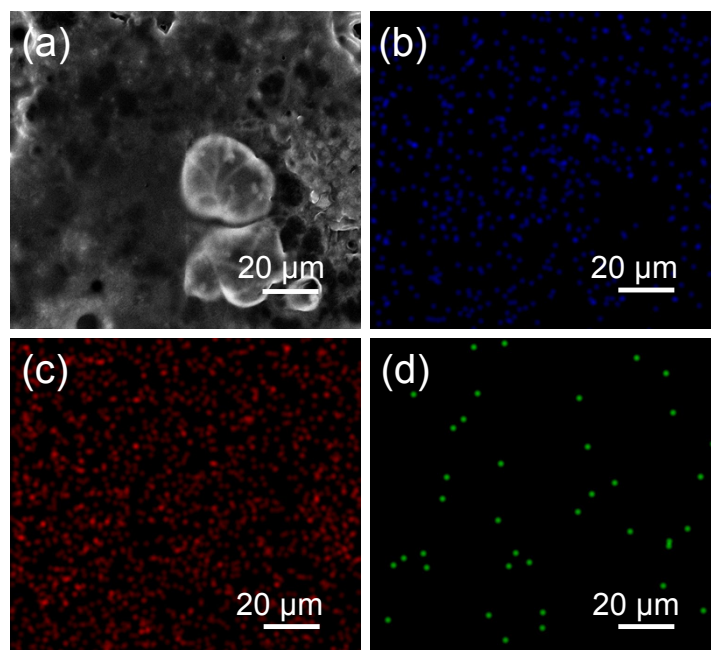


Figure S13. (a) SEM images of the lithium-metal surface morphology after 50 cycles in the DOL/TTE electrolyte before sputtering. EDS elemental mappings showing (b) F, (c) S, and (d) N signals on the lithium-metal surface.

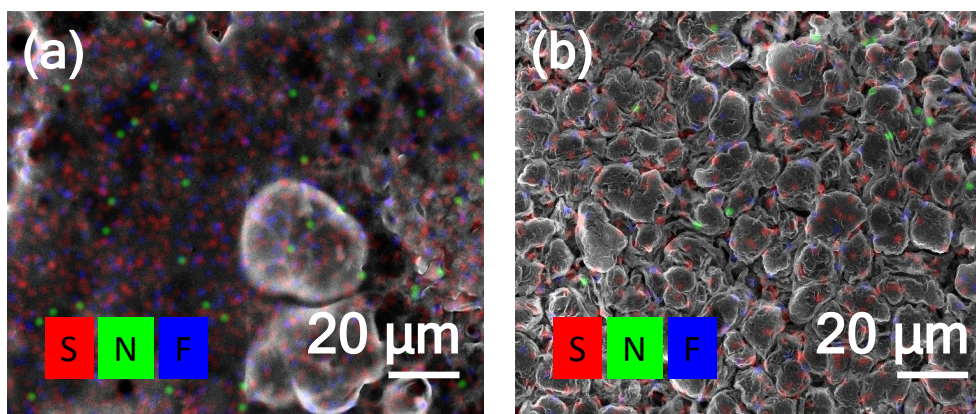


Figure S14. EDS analysis of the lithium-metal anode (a) before sputtering and (b) after sputtering for 300 s.